# Title: On the reproductive mechanisms of Gram-positive protocells

Dheeraj Kanaparthi[1,2&3*], Marko Lampe[4], Falk Hildebrand[5], Thomas Boesen[6], Andreas Klingl[7], Prasad Phapale[8], Tillmann Lueders[2&3*]& Petra Schwille[1*]

**Affiliations:**

[1]Max-Planck Institute for Biochemistry, Munich, Germany

[2]Chair of Ecological Microbiology, BayCeer, University of Bayreuth, Germany.

[3]Helmholtz Zentrum Munich, Germany

[4]Advanced Light Microscopy Facility, European Molecular Biology Laboratory, Heidelberg, Germany.

[5]Quadrum institute, Norwich, UK.

[6]Department of Biosciences, Center for Electromicrobiology, Aarhus, Denmark.

[7]Department of Biology, LMU, Planegg-Martinsried, Germany.

[8]European Molecular Biology Laboratory, Heidelberg, Germany.

**Abstract:** Bacterial protoplasts are believed to reproduce in a haphazard manner. Their unregulated method of reproduction is considered the simplest of all known forms of cell replication. In the present study, we attempted to understand the evolutionary significance and physiochemical mechanisms behind this process. Here we transformed a Gram-positive bacterium into sack of cytoplasm, incapable of regulating either its morphology or reproductive processes. As such primitive (proto)cells devoid of molecular biological processes could have been native to early Earth, we grew these cells under environmental conditions of early Earth. We then monitored these cells at regular intervals to understand if they can grow and reproduce under these conditions. In our incubations, cells exhibited a multi-stage reproductive cycle resulting in viable daughter cells. What was previously thought to be a chaotic reproductive process, could in fact be well explained from a physicochemical perspective. Both morphology and reproductive process of these cells were determined by chemical and self-assembling properties of their cell constituents rather than the information encoded in their genome. Despite its haphazard appearance, we propose that the reproductive process of bacterial protoplasts is better optimized for environmental conditions of early Earth and could be reminiscent of protocell reproductive processes.

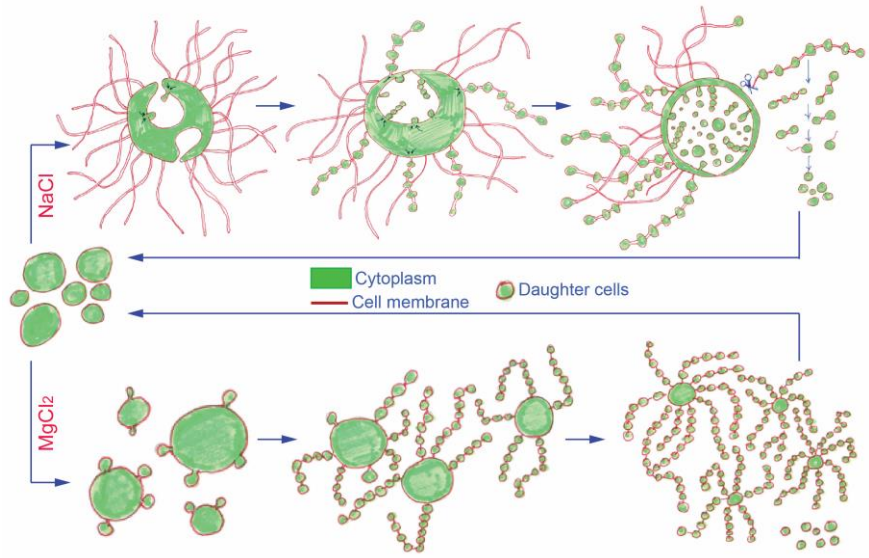

**Key words:** Protocells, Gram-positive, evolution, Archaean Eon, biophysics, cell-division, protocell reproduction, chemical evolution.

## Introduction

Theory of chemical evolution proposes that prokaryotes evolved from more primitive protocells [1]. To date most theoretical propositions on protocells, were largely a result of studying lipid vesicles with aqueous core as proxy protocells [2,3]. Despite accomplishing considerable progress in our theoretical understanding of protocells, we believe studies conducted on lipid vesicles do not represent true complexities of a living cell. To understand reproductive processes of protocells in all its complexity, we previously worked with protoplasts of Gram-negative bacteria (*R. sphaeroides*) as proxy protocells (accompanying manuscript). From this study we demonstrated that cellular reproduction could be mediated by physiochemical properties of cell constituents, similar to the theoretical propositions made from studying multilamellar lipid vesicles [3]. Nevertheless, several aspects of growth and reproduction observed in these cells was inextricably linked to the multilamellar nature of these organisms (Gram-negative bacteria with outer and inner membrane). Although, reproductive process we observed in these cells could be reminiscent of proto-Gram-negative bacteria, the question remains, how did uni-lamellar protocells (proto-Gram-positive bacteria) reproduce?

To understand reproductive process of unilamellar protocells, here we transformed Gram-positive bacteria *Exiguobacterium strain Molly* into their protoplast state, in which they are incapable of regulating either their morphology or reproductive processes. As environmental conditions [4] were known to determine physiochemical properties of cell constituents, we grew these cells (proxy-protocells) under environmental conditions of early Earth. For the

reasons mentioned in the accompanying manuscript[5–7], we used half strength tryptic soya broth (TSB) supplemented with 5-10% Dead Sea salt (DSS) at 30°C, to simulate the environmental conditions of early Earth. We then monitored these cells at regular intervals to understand if and how these cells grow and reproduce. In the below sections of the manuscript, we present an in-depth morphological transformation of *EM-P*, followed by an explanation of the physicochemical mechanisms driving such transformations.

## Results

Method of reproduction we observed in Gram-positive *EM-P* differed considerably from what we observed earlier in Gram-negative *RS-P* (accompanying manuscript). Moreover, *EM-P* reproduced by not one but by a variety of reproductive processes. In brief, *EM-P* reproduced either by forming external or internal daughter cells.

During the lag-phase, most cells were observed to have formed hollow filamentous (Figure 1A&B, open arrows; Movie S1) or spherical membrane extension (Figure 1A&B, closed arrows; Movie S2). During the early-log phase, cytoplasm was transferred from the parent cell into these spherical membrane extensions, leading to the formation of daughter cells (Figure 1C). Daughter cells then dethatched from the parent cell in a sequence of steps shown in Figure 1C-F (closed arrow). Size, shape, and number of daughter cells formed by single *EM-P* cell, varied greatly from cell-to-cell (Figure 1C-K). A noticeable pattern did not emerge over numerous repetitions. Depending on the size of the daughter cells, *EM-P* cells in this growth stage appeared to have been reproducing either by budding (Figure 1G-K) or binary fission (Figure 1D&F).

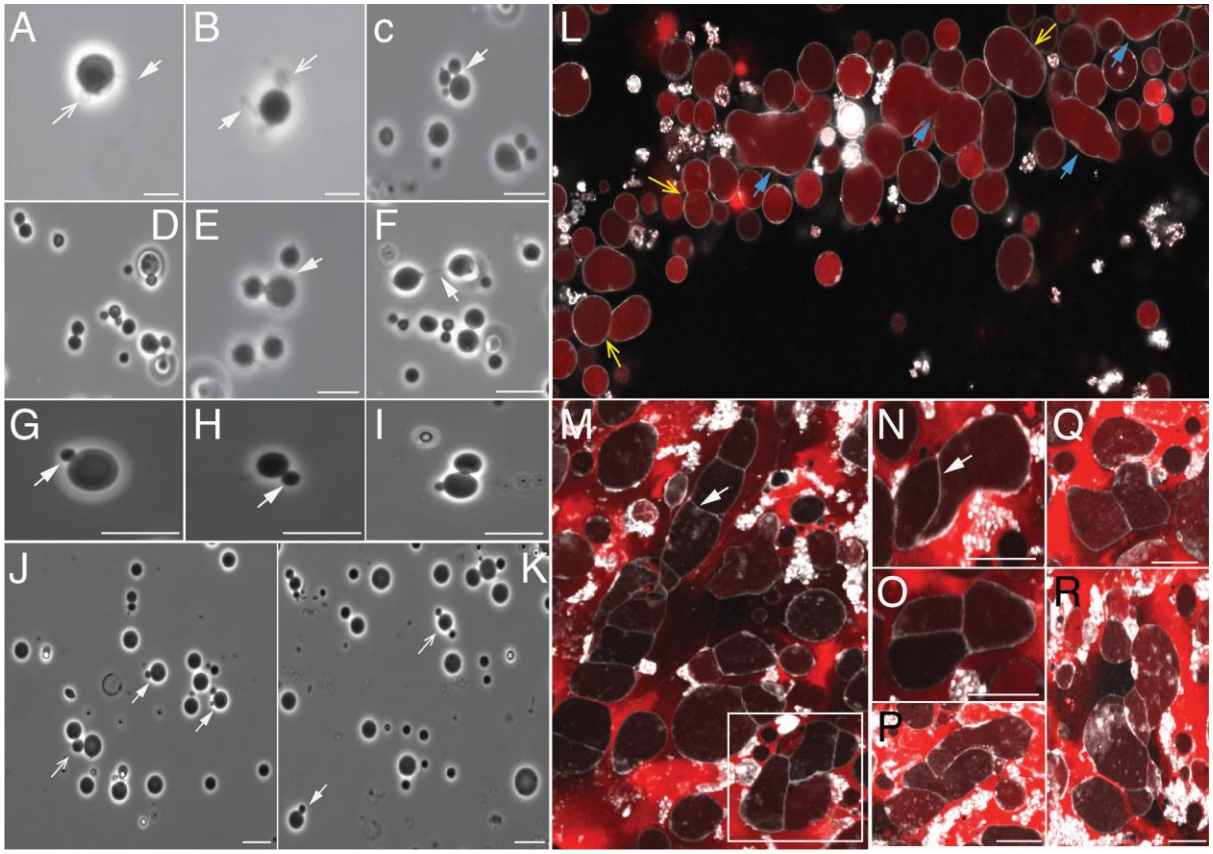


**Figure 1. Early growth stage *EM-P* cell**

Images A-F show sequential stages involved in reproduction of *EM-P* that resemble binary fission or budding. Open arrows in images A&B points to spherical and closed arrows points to filamentous membrane extensions. Images C&D show daughter cells with cytoplasm still attached (arrows) to the parent cell. Image E show, daughter cells dethatching (arrow) from the parent cell. Image F show cells in dyad, still separating from one another. Images G-K show *EM-P* with external daughter cells of different sizes. Scale bars: 10μm. Images L-R are STED microscope images of *EM-P* reproducing via formation of random morphologies. Cells in these images were stained with universal membrane stain, FM™5-95 (white) and DNA stain, PicoGreen™ (red). Blue arrows in image L points to cells expanding in random directions. Yellow arrows points to membrane septa that was being formed. M-R show later growth stages of such cell with fully formed membrane septa. Scale bars: 5μm.

During early log-phase, we also observed some *EM-P* cells reproducing via the formation of random morphologies (Figure 1L-R). These morphologies could have been a result of cytoplasm expanding in random directions. After this cytoplasmic expansion, membrane partitions were formed which compartmentalized and segregated parent cell into multiple daughter cells (Figure 1M). No uniformity was observed in the pattern of membrane septa formation (Figure 1M-R). Daughter cells formed by this process also differed widely in their size and morphology (Figure 1M-R).

By the late log and early stationary growth phase, filamentous structures formed during earlier growth stages grew in numbers (Movie S3). Unlike the lag-phase cells with one or two filamentous extensions (Figure 1A&B; Movies S1&S2), cells of this growth stage were observed to have developed multiple filamentous extensions often encompassing entire surface of the cell (Movie S3). These filamentous extensions were in a constant state of motion. Subsequently, these filamentous extensions grew in length and diameter and developed surface depressions along their length resembling tubular vesicles subjected to curvature-induced destabilization at their surface (like Rayleigh-Plateau instability) (Movie S4).

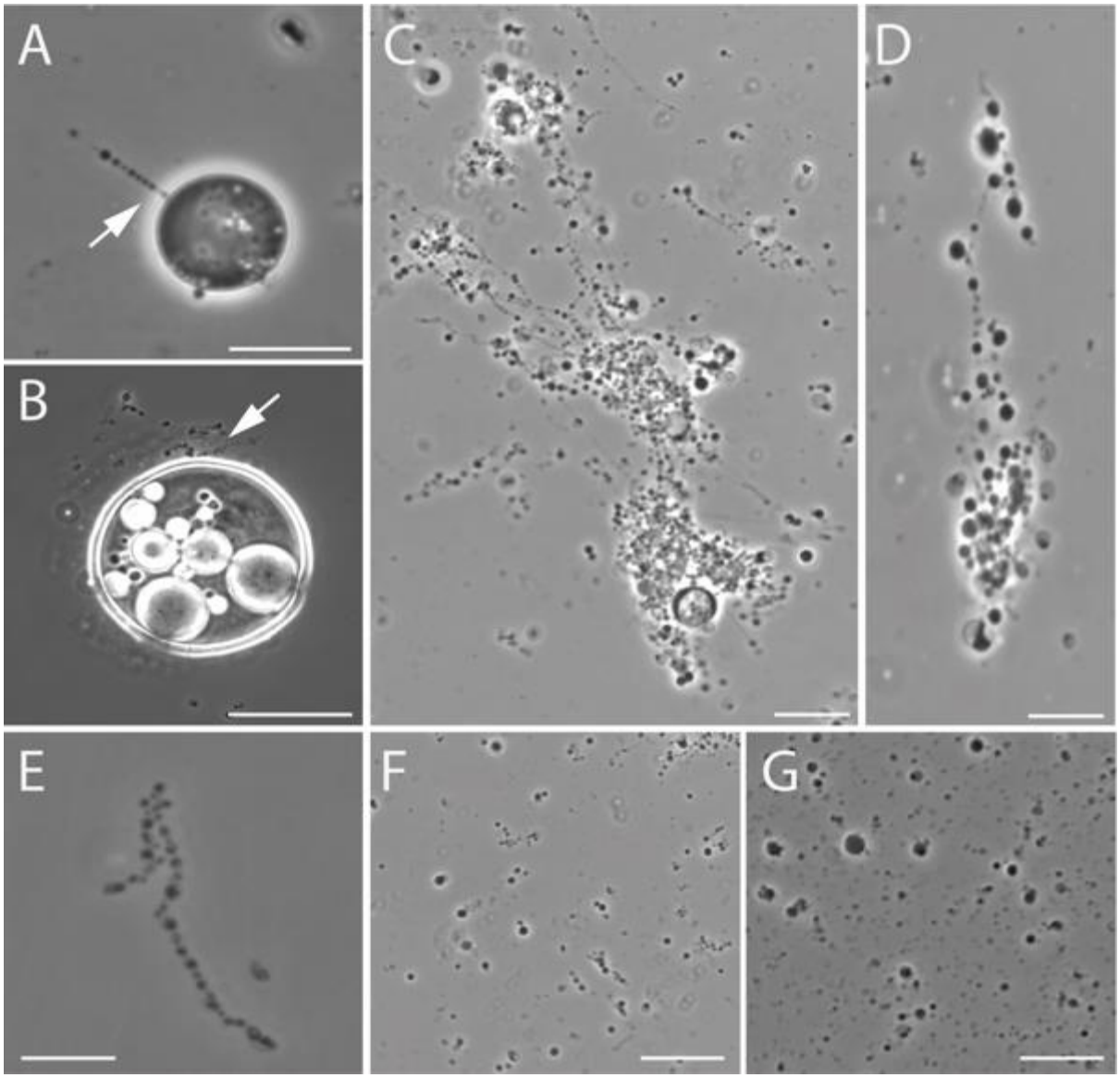


**Figure 2. Life cycle of *EM-L* reproducing via formation of extracellular daughter cells**

Images A-G show sequential stages involved in formation of a string of daughter cells (A-C, arrows) and their subsequent fragmentation into individual daughter cells (D-G). Scale bars: 10μm.

In the Subsequent growth stages cytoplasm was transferred from the parent cell into these filaments (Figure 2A). This led to the transformation of the filaments from a tubular into a "string of beads" morphology (Figure 2A-E). Over time, these filaments detached from the

parent cell and fragmented into individual daughter cells in a sequence of steps as shown in Figure 2D-G (Movies S5).

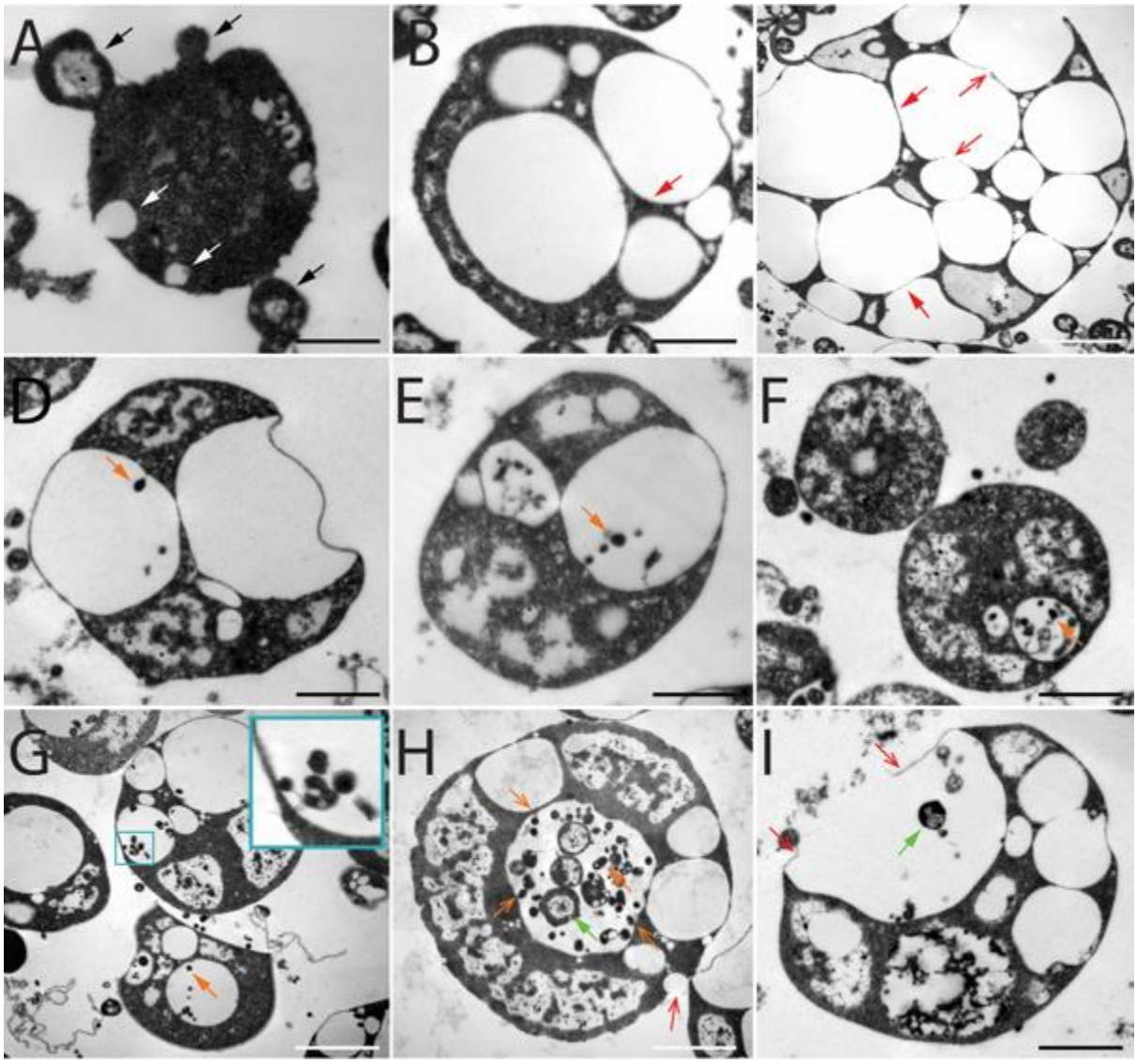


**Figure 3. Life cycle of *EM-P* reproducing via formation of intracellular daughter cells**

Images A-I are TEM images showing sequential morphological transformation of *EM-P* reproducing by formation of intracellular daughter cells. Image A shows the ongoing formation of intracellular vesicles (white arrows). Images B & C show increase in volume or numbers of intracellular vesicles within the cell. Closed red arrows points to cytoplasmic region of the cell and open red arrows points to the ruptured regions of vesicle membrane. Images D-F show the formation and growth of intracellular daughter cells (orange arrows).

Images G-I show *EM-L* cells with a mix of tiny spherical daughter cell (orange arrows) and daughter cells with intracellular vesicles (boxed region in G & green arrows in H & I). Open orange arrows in image H points to daughter cells being formed from different regions of the vesicle. Image I show the process of daughter cell release by rupture of vesicle membrane (open red arrows). Scale bars: 1μm.

The first step in reproduction via intracellular daughter cells was the formation of intracellular vesicles (Figure 3A, white arrows). These vesicles were formed by two different methods. In the first method intracellular vesicle filled with growth media were formed by a process similar to that of endocytosis (Figure 3A, white arrows). In the second method, excess membrane initially accumulated as folded lump attached to the membrane surface (Figure 4A&B). By the influx of growth media, these lumps expanded into spherical ( boxed region and arrow in Figure 4B) or filamentous vesicles (Figure 4D, arrow). Over time, filamentous vesicles gradually transformed either into a string of spherical vesicles (Figure 4D-F). Cells in this growth stage are morphologically diverse with multiple spherical (Figure 4C&F, S1), filamentous (Figure S2) or spherical intracellular vesicles interconnected by filamentous strings (Figure 4D-F & S2). Number, size, and pattern of arrangement of the vesicles within a cell widely varied form cell-to-cell and no specific pattern emerged over multiple repetitions (Figure S1).

Daughter cells were formed into the vesicles by a process similar to budding (Figure 3D). Vesicle membrane underwent a positive curvature to form bud-like structures extending into the vesicles (Figure 3D, orange arrow). Multiple such structures were observed within a single vesicle originating from different points (Movie S6). These buds either dethatched

from the vesicle surface into an individual daughter cell (Figure 3H) or grew into a string of daughter cells

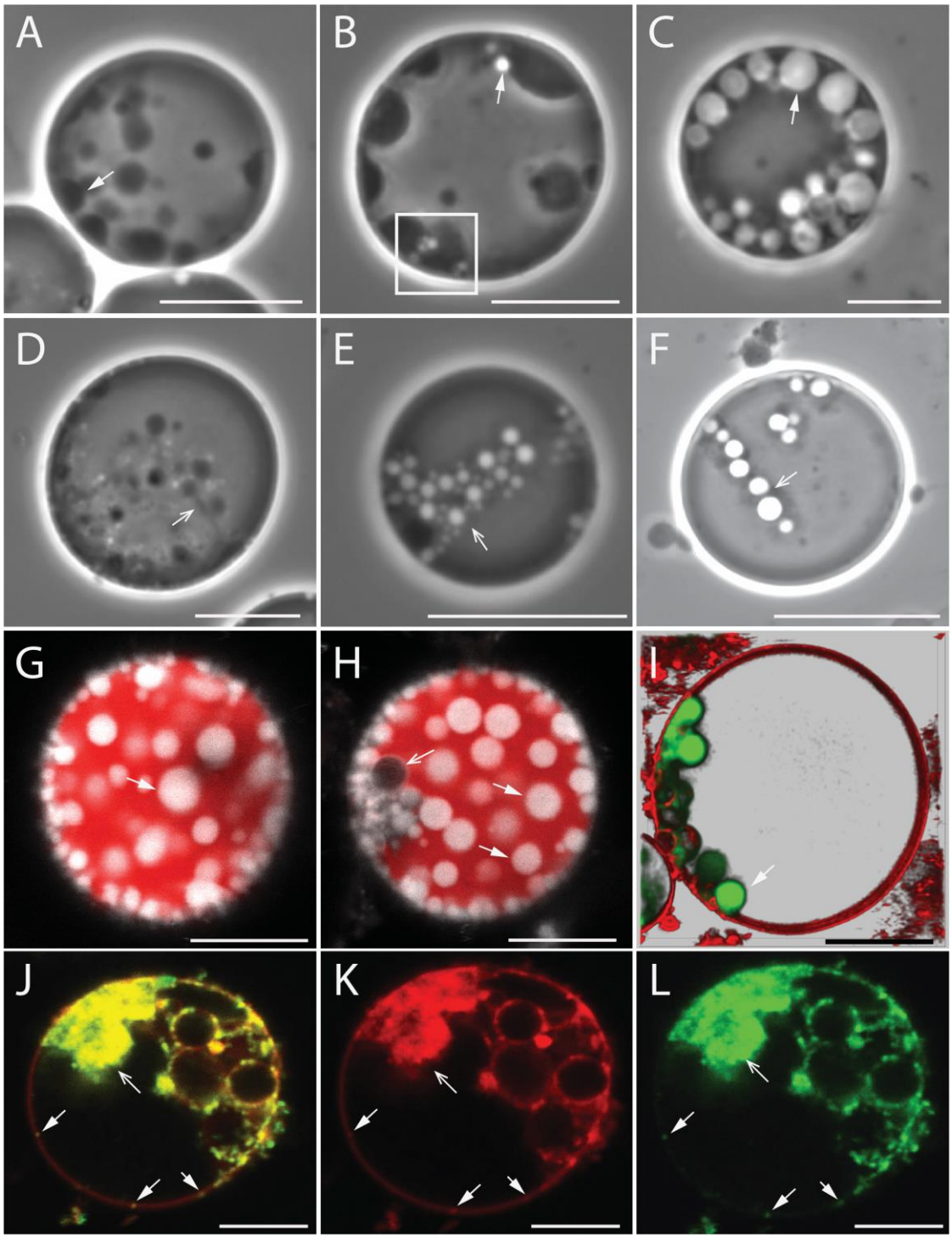


**Figure 4. Sequential steps involved in formation of intracellular vesicles**

Images A&B show *EM-P* cells with excess membrane accumulated as a lump attached to the cell membrane (arrows). In the subsequent growth stages growth media was transferred into

these membrane lumps (arrows & boxed region), leading to their transformation into individual spherical vesicles (C). Image D show initial expansion of membrane lumps into filaments (arrows). Images E&F show inflation of these filaments into string of vesicles (arrows), by influx of growth media. Images G&H show cells with intracellular membrane lumps. Cells in these images are stained as mentioned in Figure 1. Image I show these intracellular membrane lumps and vesicles were exclusively composed of $L_d$ membrane. Image J-L show STED microscope images of *EM-P* cell undergoing membrane phase separation. Cells in these images were stained with universal membrane stain, FM™5-95 (red) and membrane stain that specifically stains $L_d$ membrane, *FAST*™ Dil (green). Arrows in these images point to tiny patches of $L_d$ membrane (≈ 180nm) in cell surface. Open arrows in these images point to large clumps of coalesced $L_d$ membrane within the cell. Scale bars: 5μm.

(Figure 3E, orange arrow) and then fragmented into multiple daughter cells (Figure 3H). In contrast to the daughter cells that were formed out of the cell, budding process and cytoplasmic transfer happened simultaneously for internal daughter cells (Figure 3D&E). Daughter cells formed by this process were tiny (0.2 - 1μm in diameter) in comparison to the parent cells (Figure 3H) and are highly mobile (Movie S7). Due to gradual transfer of cytoplasm from parent to daughter cells (Figure 3D, E & S3), we observed *EM-P* parent cells that were depleted in their cytoplasmic content (Figure 3B, C & S3). These cells were hollow with a single (Figure S3) or variable number of intracellular vesicles (Figure S4) containing highly motile daughter cells (Movie S7). Daughter cells were released into the surrounding media by rupture of cell or vesicle membrane (Figure 3I, red arrows & S4G&H, closed arrows). The final growth stage of *EM-P* was characterized by the presence of cells with all

the above-described morphologies along with considerable amount of membrane debris (Figure S5).

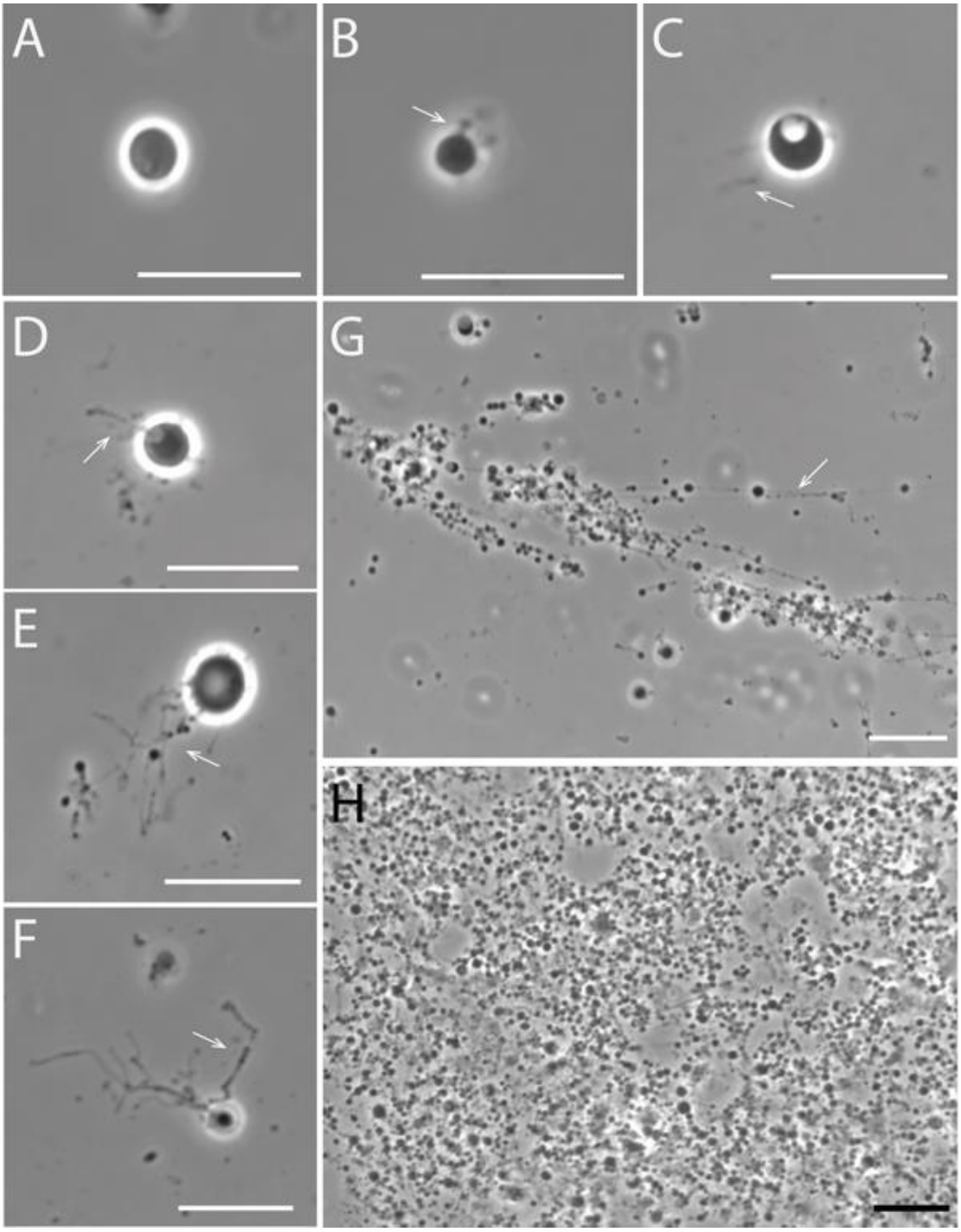


**Figure 5. Phase-contrast images of *EM-P* reproducing when grown in $MgCl_2$**

Images A-H sequential morphological transformation of *EM-P* when grown in the presence of 7% $MgCl_2$. Image A show *EM-P* cells from 7%DSS-TSB that were inoculated into 7%

$MgCl_2$-TSB media containing. Cells developed hollow filamentous membrane extensions (C-arrows). Cytoplasm was gradually transferred into these filamentous extensions (D). Images D-E show formation of daughter cells within these filaments. Images G & H show stationary-phase *EM-P* cells. Scale bars: 10μm.

Given the chemical composition of growth media and physical forces influenced the morphology of Gram-negative protoplasts in our previous study, we also tested their influence on the morphology and reproductive process of *EM-P*. *EM-P* exhibited a trend similar to what was previously observed in *RS-P* when grown in KCl and $MgCl_2$ (accompanying manuscript). Cells grown in KCl were similar in size and morphology to the cells grown in DSS. In contrast, cells grown in $MgCl_2$ were significantly smaller in sizes in comparison to cells grown in equivalent concentrations of DSS (Figure 5, S6, S7 & Movie S8). Apart from the differences in the sizes, a higher portion of cells grown in KCl were observed to be reproducing via formation of internal daughter cells. Similarly, when grown in $MgCl_2$, diameter of the cells was restricted to 0.5-2μm and mostly reproduced by forming extracellular daughter cells (Figure 5C-F & S6). Also, in contrast to the above-described reproductive process, daughter cells formed by this process did not detach from the parent cell immediately. Over time, they formed an entangled web of strings with spherical daughter cells (Figure 5H).

To understand the influence of turbulent multiaxial elongational flow conditions on *EM-P*'s morphology and reproductive processes, we grew *EM-P* on an orbital shaker. Under these growth conditions, *EM-P* reproduced exclusively by a process resembling binary fission. None of the above-described morphologies like large cells with intracellular vesicles, strings

of daughter cells or membrane debris was observed. Most cells observed under this type of growth resemble in size and shape to the ones shown in Figure 1A-K.

## Discussion

Repertoire of morphologies and diverse reproductive pathways of *EM-P* could be explained by the biophysical properties of its cell constituents and an unorderly molecular biological regulatory mechanism [8]. Hollow spherical and filamentous extensions (Figure 1A&B) extending into or out of the cell and intracellular membrane lumps (Figure 4A&B) observed during the lag-phase, could have formed due to slower rate of cytoplasmic volume increase in-comparison to lipid synthesis [9]. A similar phenomenon of excess lipid synthesis was reported in bacterial protoplasts by earlier studies [9]. Like explained in case of *RS-P* (accompanying manuscript), formation of such structures could be explained by ADE theory [10,11]. ADE theory states that when the area of the vesicle is smaller than that of the expected value, vesicles undergo shape deformation, as a mechanism of accommodating excess membrane. Invagination of membrane, leading to the formation of buds and filamentous structures we observed in *EM-P* was in-tune with ADE theory and what was previously observed in lipid vesicles undergoing osmotic shrinkage [10,11]. A condition that resembles *EM-P* cells with excessive membrane (Figure 4A, B & Movie S3).

Formation of external and inter membrane structures could also be explained by the hypothesis proposed by Lipowsky & Jülicher [12,13]. It was proposed that, phase-separated membranes tend to minimize interfacial energy at the phase boundary to attain a thermodynamically stable state. They do so by forming an out of plane membrane deformation, which gradually transforming softer liquid disordered ($L_d$)-membrane into a bud

(Figure 4I). Earlier studies hypothesized that $L_d$-membrane most likely undergoes budding due to their low bending rigidities and high spontaneous curvature [14]. Despite these propositions, to date membrane phase-separation has been only reported in lipid vesicles. To the best of our knowledge, ours is the first study to provide visual evidence of membrane phase-separation in live cells (Figure 4I-L). In accordance with this theory, cell membrane underwent phase-separation into $L_d$ and $L_o$ membrane fractions (Figure 4 J-L). $L_d$ membrane initially appeared as small patches on the cell surface, less than 180nm in diameter (Figure 4 J-L). As area of $L_d$ membrane increased, it underwent budding due to an increase in the line tension at the phase boundary[15]. Nevertheless, some deviations from this expected behavior were observed. First, there was the difference in the direction of budding. Contrary to the predictions, we observed $L_d$-membrane undergoing a negative (into the cell), rather than positive (out of the cell) curvature (Figure 4I). Second, despite its higher bending rigidity, liquid ordered ($L_o$)-membrane too underwent deformation out of the cell (Movie S8). Intriguingly, all positive (out of the cell) membrane deformations were exclusively composed of $L_o$-membrane and all negative membrane deformations (into the cell) were exclusively composed of $L_d$-membrane (Figure 4I & Movie S9).

Direction and physical nature of a membrane undergoing budding could be explained by its lipid composition, bi-layer asymmetry, concentration of sterols and the nature of the aqueous core. Bacia *et al* studied the influence of cholesterol and related sterols on budding [16]. Despite higher bending rigidities, this study showed that some sterols can induce budding of $L_o$-membrane instead of $L_d$-membrane. Prokaryotes are known to lack sterols like cholesterol and its derivatives. Nevertheless, prokaryotes are known to have functional analogues of cholesterol, like hopanoids [17]. Properties of these compounds in membrane phase-separation and budding were rarely investigated. Apart from these studies, invagination of $L_o$-membrane

was also reported to happen during the osmotic shrinkage of vesicles [11] and was also observed in-vivo [18].

Nature and direction of the membrane invagination could also have been determined by aqueous core (cytoplasm) and media surrounding the cell [14]. Studies showed that when aqueous core of the lipid vesicles (LV's) underwent phase-separation (not the membrane) according to their densities, vesicle membrane too underwent phase-separation [14,19]. The denser part of the aqueous core was observed to be associated with $L_d$ and the lighter part was surrounded by $L_o$-membrane. This could explain invagination of $L_d$-membrane into the cell, given the higher densities of cytoplasm (~17-35 wt% molecules). Preference of $L_o$-membrane to the comparatively less dense media (~6-7 wt% molecules), could have led to $L_o$-membrane undergoing positive curvature i.e., out of the cell (Figure 4I & Movie S9).

Apart from the differences observed in the physical properties of membrane that underwent positive and negative invagination, we also observed differences in the morphologies of these membrane extensions over the course of *EM-P*'s growth. During log-phase, most cells were observed to have multiple, relatively short membrane extensions (Figure 1A&B, Movie S1 & S2). On the other hand, we observed most stationary growth-stage cells having a long filamentous (Movie S10) or thick tubular extension (Movie S4). Similar formation of membrane extensions was reported from lipid vesicles [14]. It was shown that morphology and number of membrane extensions from a single vesicle is determined by the rate of lipid transfer from the vesicle into these filamentous extensions. A slower rate of transfer led to the formation of membrane extensions from multiple sites. Relatively faster rate of lipid transfer, led to the formation of fewer but longer filaments. In case of *EM-P* we argue that rate of lipid transfer is dependent on its growth kinetics. During log-phase when the growth rate is high, cytoplasmic volume increase kept pace with the membrane synthesis i.e., less membrane was

available for formation of hollow filamentous extensions. Hence during this growth stage, it is thermodynamically favorable for the membrane to form invaginations at multiple sites on its surface (Movie S1 & S2). At later growth-stage, when the ratio of cytoplasmic volume increase to amount of excess membrane is low i.e., more membrane area is available for the formation of hollow filamentous extensions. It is energetically favorable for already existing filamentous structures to undergo extensions (Movie S10) rather than forming new membrane invaginations on its surface. Nevertheless, no uniformity was observed in the thickness or the length of the filaments (Movie S3, S4 & S10). Large differences were also observed in the diameter of the filamentous extensions, which ranged between 0.1 to 1μm. A similar variability in the diameter of filamentous extensions was reported from earlier studies on LV's [14]. Like the LV's, we presume these differences originated due to asymmetry in the size of the inner and outer leaflet lipids in the membrane.

Formation of external daughter cells happened by the transfer of cytoplasm from the cell into these membrane extensions. Subsequent transformation of filaments from tubular morphology to a "string of beads" could be explained by the lower volume of cytoplasm that was transferred into the filaments compared to the volume of the filament [14]. Under such conditions, tubular membrane structures were known to undergo deformations resembling Rayleigh-Plateau like instability (Movie S4) [14]. The excess membrane within these tubular structures transformed into tethers connecting adjacent daughter cells (Figure 2C&D). Rupture of these tethers led to the detachment of these strings from the cell surface and their fragmentation leading to the formation individual daughter cells (Movie S5).

One key aspect of the cell-cycle is reproduction by fission of the parent cell into metabolically viable daughter cells (Movie S5). Archiving fission among lipid vesicles has been the primary focus of multiple studies and is of key importance in enhancing our

understanding of most primitive cell replication processes [20] and building autonomously replicating synthetic cells [21,22]. Previous studies archived fission either by mechanical means [23] or by encapsulating protein involved in cell division [24] or by incorporation of lipids into the vesicles [3]. Given that *EM-P* was cultured under static conditions and has an ineffective molecular biological regulatory processes [8], we presume that force driving the fission process was primarily physiochemical in nature. During all the growth stages we observed that cells were in a constant state of oscillation (Movie S7 & S11). We presume these oscillations were a result of differences in osmolarities [25], chemical composition or concentrations of different compounds on either side of the membrane [26]. All these factors together with the virtue of processing an internal metabolism [27] were hypothesized to generate surface deformations, ultimately leading to cell-fission. We also observed movement of intracellular constituents within *EM-P* (Movie S11), which could also have contributed to surface oscillations observed in *EM-P*. This constant state of oscillation could have led to the rupture of membrane tethers connecting daughter cells led to the formation of individual daughter cells (Movie S5). Like observed in *RS-P*, we do not presume that proteins involved in canonical cell replication process are resulted in surface oscillations. Treatment of *EM-P* with bactericidal chemicals like sodium azide (0.3%)[28] or 0.5% formaldehyde[29] which inactivates intracellular proteins did not result in a static cell. Surface oscillations of *EM-P* could only be halted by equilibrating cytoplasmic components with the outside by creating pores in the membrane using Triton X100 (0.5%)[29], suggesting that asymmetric conditions on either side of the cell membrane resulted in the oscillation of the cell.

*EM-P*'s lifecycle we presented above is consensual rather than literal. Within a single growth stage cells usually are a mixture of different morphologies. No uniformity was observed either in size, number of internal vesicles (Figure S1&S2), filamentous extensions on the cell

(Movie S3, S5 & S10) or in the sizes of the daughter cells (Figure 2 & S3 F&G, S6 & S7). We presume these variations could be explained by differences in the growth rates [14] of individual cells and everchanging aspect ratio of the cell (Movie S11) [30,31], as discussed in detail in the accompanying manuscript.

Considerable differences in morphologies observed between *EM-P* cells grown in the presence of KCl or $MgCl_2$, could also be due to reasons we proposed for *RS-L* (accompanying manuscript). In-brief, nature of interactions between cations and phospholipid head groups was known to influence elasticity of the cell membrane [26]. Earlier studies showed an increase in the fluidity of the membrane in the presence of monovalent cations like potassium and decrease in their fluidity in the presence of divalent cations [32]. Easier expansion of cell membrane in incubations contain DSS and KCl [26] could have facilitated the formation relatively larger cells and reduced elasticity of the membrane in the presence of $MgCl_2$ could have led to the formation of smaller cell. The reasons for the reproducing predominantly via extracellular daughter in the presence of $MgCl_2$ and predominantly via extracellular daughter cells in the presence of KCl is currently unclear. Nevertheless, a similar phenomenon of intracellular vesicle formation in the presence of KCl was reported from phospholipid vesicles [26].

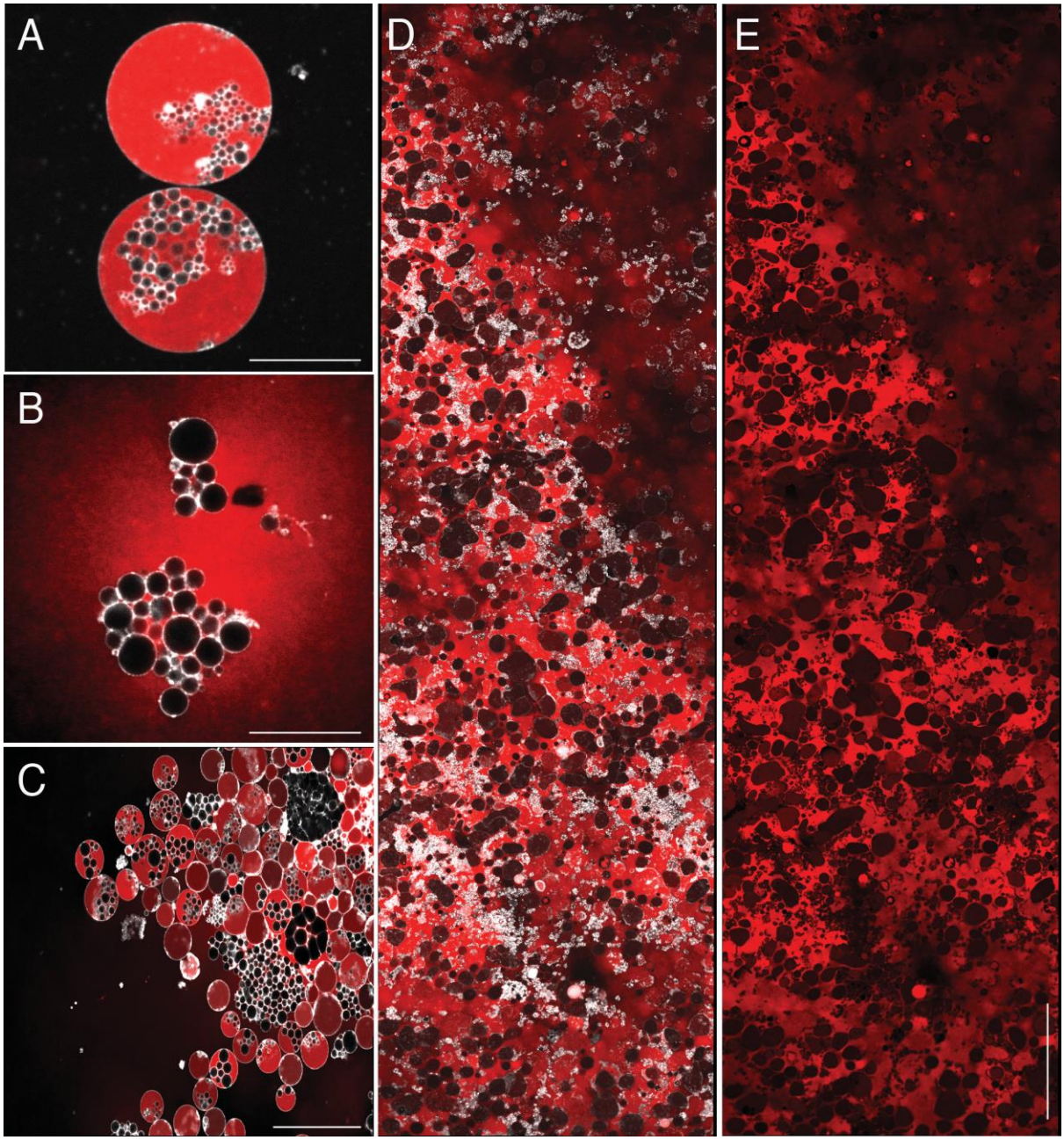


**Figure 6. Leakage of cell constituents during *EM-P*'s reproduction**

Image A shows intact *EM-P* cells. Cells in these images were stained with universal membrane stain, FM™5-95 (white) and DNA stain, PicoGreen™ (red). Image B show lysis of cells and release of intracellular constituents. Image C show early growth stage cells with undergoing lysis. Images D&E show cells in their log phase of growth. Image E only show the DNA channel. Scale bars: 10μm.

Despite successfully reproducing by simplest of mechanisms, the efficiency by which these cells reproduced was considerably lower than the cells in their native form (Figure 6 & S8). This is evident from the considerable amount of extracellular DNA in our incubations (Figure 6 & S8), suggesting cell lysis and leakage of intracellular constituents. *EM-P* cells undergoing gentler or explosive lysis and release of DNA was observed during all growth stages (Figure S6, S9 & Movie S13). To the best of our knowledge, such explosion of cells has never been reported in living cells. However, similar rupture of lipid vesicles by two different mechanisms was previously known, either by osmotic pressure created by Reactive Oxygen Species (ROS) upon exposure to light [33] or by interactions between DNA and lipid head groups [34]. In fact, bacterial protoplasts were known to produce high amount of ROS [35]. Hence, there exists a possibility that lysis observed in *EM-P* could have been induced by ROS. Lysis of cells could also have been photo-induced during the imaging process (by confocal or a STED microscope). Nevertheless, we also noticed end products of cell explosion (extracellular DNA) when the cells were grown in the dark and when *EM-P* was grown under anaerobic conditions, to prevent the formation of ROS. Therefore, we presume that this process could have been mediated by interactions between DNA and the cell membrane [34].

The efficiency of reproduction in *EM-P* was also dependent on the growth conditions. Less leakage of cell constituents was observed when cells were grown in the presence of $MgCl_2$, than in other salts (Figure S8). Despite this wastefulness, all our incubations resulted in viable daughter cells (Figure 7). Smaller daughter cells that were separated from membrane debris and other larger daughter cells by passing through 0.44μm filter showed presence of DNA, cytoplasmic activity (Figure 7) and always resulted in growth when transferred into fresh media.

Significantly less leakage of cell constituents was observed when *EM-P* was grown on an orbital shaker than under static conditions (Figure S8). These observations suggest that reproductive efficiency of *EM-P* like cells could be more efficient in natural environments than what was observed in our static incubations. This could be especially true for Archaean Eon Earth, as most life during this time was restricted to costal marine environments [36,37], where cells will be subjected to constant motion by tidal waves.

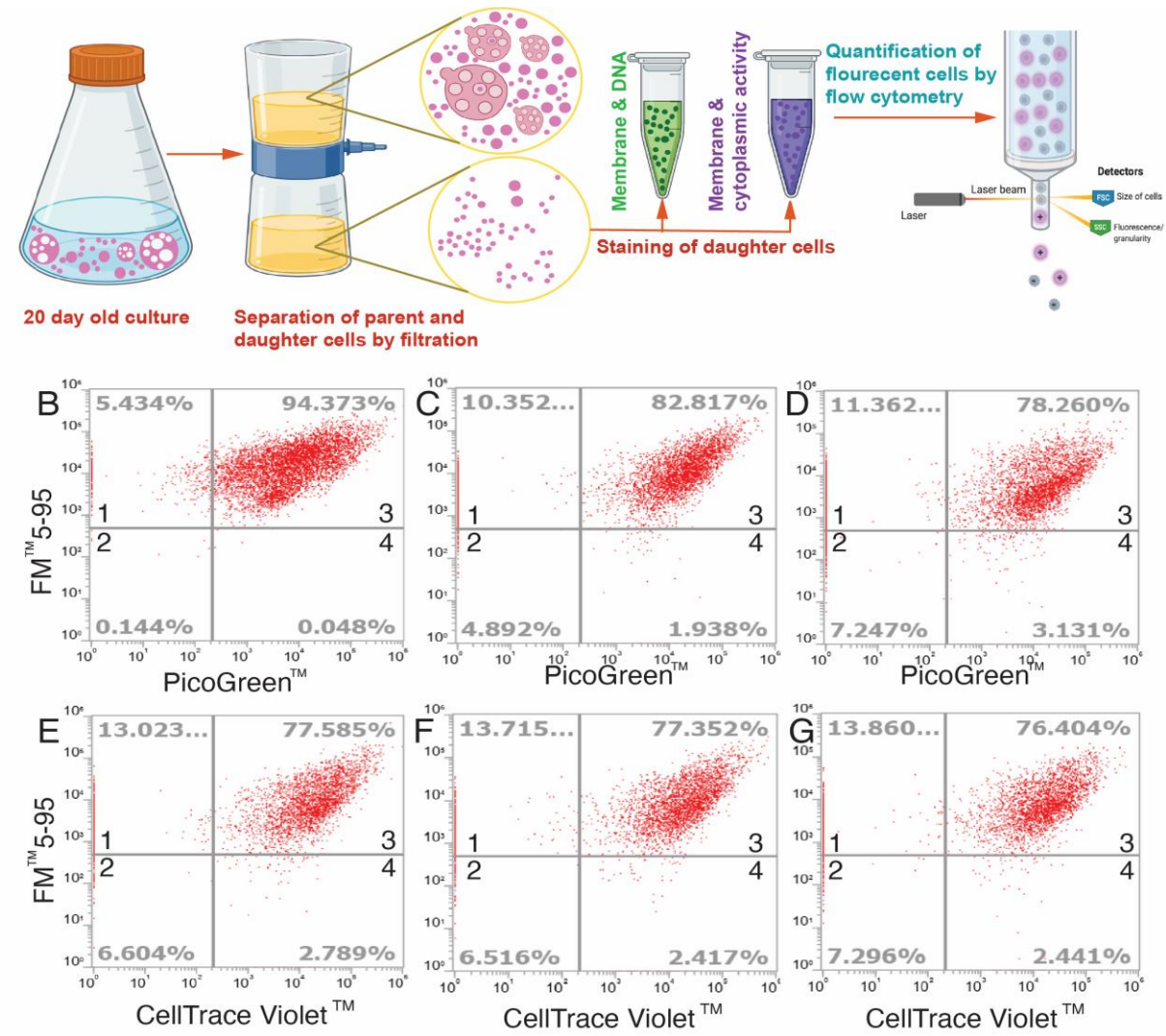


**Figure 7. Viability of daughter *EM-P* cells**

Panel A show the workflow of the experiment. Images B-G show flowcytometry plots. Quadrants 1, 2, 3 & 4 in each plot represent the percentage of cells stained with only FM™5-95 (1), cells stained with only PicoGreen™ (2), cells stained by both FM™5-95 & PicoGreen™ (3) and cells that weren't stained either by FM™5-95 & PicoGreen™ (4). Images B-D show triplicate plots of *EM-P* cells grown in 5%$MgCl_2$-TSB and images E-G show triplicate plots of *EM-P* cells grown in 5%DSS-TSB.

Despite all the unpredictability and a chaotic mixture of morphologies (in terms of size and number of intracellular vesicles) within any given growth stage, the end morphologies of *EM-P* are largely restricted to morphologies we presented in the manuscript. Moreover, no morphological overlap was observed between Gram-negative *RS-P* (accompanying manuscript) and Gram-positive *EM-P*. Hence, we assume that apart from the physicochemical properties of the growth media and cell constituents; membrane architecture played an important role in determining cell morphology. Mechanisms of reproduction we observed in *EM-P* is also similar to reproductive processes observed in minimal cells that were a result of top-down synthetic biology approach [38] (Figure S10 & S11) and computer simulations of protocell reproduction process [39] (Figure S12).

**Bacterial protoplasts as analogues of proto-life**

From the time of life's origin, until the beginning of evolution by natural selection (Darwinian evolution), living organisms were believed to have undergone changes over time or adapted to a new environment by a process known as chemical evolution [1,40]. During this time organisms are were presumed to be primitive and methods by which they regulated their morphology and reproduction were determined by physiochemical properties of their cell

constituents and environmental conditions [41] rather than by complex molecular biological processes. Prior to our study, methods by which they harnessed self-organization properties of cell constituents to mediate these processes like reproduction has not been experimentally demonstrated. Nevertheless, our proposal that protocell reproduced by above-described processes is predicated on three key conditions. First, primordial Earth's oceans should have salt content of 5-10% w/v. Second, the membranes of these protocells should have been of diverse phospholipid composition. Third, by the time the above-described processes became prevalent, protocells should have evolved an internal metabolism.

Saline (above 5%wt/vol) environmental conditions are required to mediate the above mentioned reproductive processes as a state of osmotic in-equilibrium between the cells and the surrounding [25,26] is required to keep cells in a constant state of oscillation (Movies S1 - S11). Hence, we presume asymmetric conditions on different leaflets of the membrane have played an important role in the mediating cell-division. Even in the presence of an osmotic in-equilibrium, such a state could only be maintained for a prolonged period, only if the membranes are composed of phospholipids rather than considerably more permeable lipid membranes [42]. Cell membranes of diverse phospholipid composition were also necessary to resist precipitation or crystallization of phospholipids and establish a lateral heterogenicity [43,44]. Due to the impermeability of phospholipid membranes to polar compounds, we assume that cells reproducing by these possesses should possesses an internal metabolism [42]. Hence, we propose that cells reproducing by above-described processes represent an evolutionarily a more advanced state of protocell, that have evolved metabolic processes for energy conservation but have not yet evolved mechanisms of regulating their morphology and reproductive processes.

Higher salinities of the Archaean oceans [7] and their significance for the origin of life was proposed by earlier studies [45]. The presence of phospholipid in the protocell membrane is also a possibility, given Fisher-Tropsch process was shown to synthesize phospholipids [46]. Although in-theory, environmental conditions of early Earth seems to be conducive for the above described processes to happen [7], arguing that protocells possessed an internal metabolism and their membranes were composed of diverse phospholipids, first requires us to provide an empirical evidence for the existence of such cells on early Earth. Unlike other theories on evolution, existence of protocells has not been proven empirically. Hence, we looked into the fossil record of early Earth (Archaean Eon microfossils) for possible existence of cells morphologically similar to the ones we observed in this study [37,47,48]. Extensive morphological comparison of microfossils with that of cells from our study, showed beyond a reasonable doubt that cells reproducing by the processes we described here, indeed existed on early Earth. Elemental and isotopic signature of these microfossils suggest that these cells were metabolically active [37,49], and their cell membranes exhibited lateral heterogenicities [50], like observed in *EM-P* and *RS-P* [51]. In-depth comparison of microfossil with *RS-P* and *EM-P*, in-terms of their morphology, chemical and isotopic compositions is beyond the scope of the current manuscript and is presented as a subsequent manuscript [51].

In conclusion, our study overturns the current assumption that bacteria reproduce in a haphazard manner in the absence of a functioning molecular biological process. Here we demonstrate that cells with internal metabolism are inherently capable of reproduction, leading to the formation of viable daughter cells. This process of reproduction is mediated by physiochemical properties of cell constituents, especially membrane phase-separation and environmental conditions that determine these properties. To the best of our knowledge, ours is the first study to provide visual evidence for the existence of phase-separated membrane in

living cells and evolutionary significance of such process. Although efficiency of reproduction was lower than that of the cells with a peptidoglycan wall, under certain environmental conditions, bacterial protoplasts reproduced with nearly similar efficiency. By studying these cells under environmental conditions of early Earth, we propose that primitive cells (protocells), devoid of molecular biological mechanisms should have reproduced by these processes. In our subsequent work we were able to demonstrate from the fossil record that this mechanism of reproduction is not merely theoretical, but protocells in-deed reproduced by these processes.

**Associated content:** Supplemental figures; Supplementary movies, Methods and Materials and Supplementary references

**Author information:** Lead contact, kanaparthi@biochem.mpg.de

**Present address:** Max-Planck Institute for Biochemistry, Munich, Germany

**Notes:** The authors declare no competing financial interest.

**Author contributions:** DK conceived the work with input from TL, BZ, ML & PS. DK performed laboratory experiments. AK did TEM imaging. DK & ML performed confocal super-resolution light microscopy imaging. DK coordinated work between the authors. DK wrote the manuscript with input from TL, BZ, ML, AK & PS. This research was funded by the European Research Council (ERC), grant agreement 616644 (POLLOX) to TL.

**Acknowledgments:** We gratefully acknowledge Ralf Conrad for his input throughout the work. We would like to thank Gabriella Berthal and Markus Oster for excellent technical support. We would also like to thank Advanced Light Microscopy Facility at EMBL, Heidelberg, Ulf Schwartz from Leica Microsystems and other members of Ecological microbiology laboratory for their support throughout the work. We thank Jan-Hagen Krohn for critical reading of the manuscript.

**Declaration of interests:** The authors declare no competing interests.

## References

(1) Oparin, A. I. Chemistry and the Origin of Life. *R. Inst. Chem. Rev.* **1969**, *2*, 1-12.

(2) Hanczyc, M. M.; Fujikawa, S. M.; Szostak, J. W. Experimental Models of Primitive Cellular Compartments: Encapsulation, Growth, and Division. *Science.* **2003**, *302*, 618–622.

(3) Zhu, T. F.; Szostak, J. W. Coupled Growth and Division of Model Protocell Membranes. *J. Am. Chem. Soc.* **2009**, *131*, 5705.

(4) Blöchliger, E.; Blocher, M.; Walde, P.; Luisi, P. L. Matrix Effect in the Size Distribution of Fatty Acid Vesicles. *J. Phys. Chem. B* **1998**, *102*, 10383–10390.

(5) Blake, R. E.; Chang, S. J.; Lepland, A. Phosphate Oxygen Isotopic Evidence for a Temperate and Biologically Active Archaean Ocean. *Nature* **2010**, *464*, 1029–1032.

(6) Catling, D. C.; Zahnle, K. J. The Archean Atmosphere. *Sci. Adv.* **2020**, *6*, eaax1420.

(7) Knauth, L. P. Salinity History of the Earth's Early Ocean. *Nature* **1998**, *395*, 554.

(8) Leaver, M.; Dominguez-Cuevas, P.; Coxhead, J. M.; Daniel, R. A.; Errington, J. Life without a Wall or Division Machine in Bacillus Subtilis. *Nature* **2009**, *457*, 849-853.

(9) Mercier, R.; Kawai, Y.; Errington, J. Excess Membrane Synthesis Drives a Primitive Mode of Cell Proliferation. *Cell* **2013**, *152*, 997–1007.

(10) Yanagisawa, M.; Imai, M.; Taniguchi, T. Periodic Modulation of Tubular Vesicles Induced by Phase Separation. *Phys. Rev. E - Stat. Nonlinear, Soft Matter Phys.* **2010**, *82*, 051928-1-9

(11) Yanagisawa, M.; Imai, M.; Taniguchi, T. Shape Deformation of Ternary Vesicles Coupled with Phase Separation. *Phys. Rev. Lett.* **2008**, *100*, 148102-4.

(12) Lipowsky, R. Budding of Membranes Induced by Intramembrane Domains. *J. Phys. II* **1992**, *2*, 1825-1840.

(13) Jülicher, F.; Lipowsky, R. Domain-Induced Budding of Vesicles. *Phys. Rev. Lett.* **1993**, *70*, 2964-2967.

(14) Liu, Y.; Agudo-Canalejo, J.; Grafmüller, A.; Dimova, R.; Lipowsky, R. Patterns of Flexible Nanotubes Formed by Liquid-Ordered and Liquid-Disordered Membranes. *ACS Nano* **2016**. *10*, 463-474.

(15) Baumgart, T.; Hess, S. T.; Webb, W. W. Imaging Coexisting Fluid Domains in Biomembrane Models Coupling Curvature and Line Tension. *Nature* **2003**, *425*, 821-824.

(16) Bacia, K.; Schwille, P.; Kurzchalia, T. Sterol Structure Determines the Separation of Phases and the Curvature of the Liquid-Ordered Phase in Model Membranes. *Proc. Natl. Acad. Sci. U. S. A.* **2005**. *102*, 3272-3277

(17) Sáenz, J. P.; Grosser, D.; Bradley, A. S.; Lagny, T. J.; Lavrynenko, O.; Broda, M.; Simons, K. Hopanoids as Functional Analogues of Cholesterol in Bacterial Membranes. *Proc. Natl. Acad. Sci. U. S. A.* **2015**. *112*, 11971-11976.

(18) Conner, S. D.; Schmid, S. L. Regulated Portals of Entry into the Cell. *Nature*. **2003**, *422*, 37-44.

(19) Li, Y.; Lipowsky, R.; Dimova, R. Membrane Nanotubes Induced by Aqueous Phase Separation and Stabilized by Spontaneous Curvature. *Proc. Natl. Acad. Sci. U. S. A.* **2011**. *108*, 4731-4736.

(20) Pelletier, J. F.; Sun, L.; Wise, K. S.; Assad-Garcia, N.; Karas, B. J.; Deerinck, T. J.; Ellisman, M. H.; Mershin, A.; Gershenfeld, N.; Chuang, R. Y.; Glass, J. I.; Strychalski, E. A. Genetic Requirements for Cell Division in a Genomically Minimal Cell. *Cell* **2021**, *184*, 2430-2440.

(21) Olivi, L.; Berger, M.; Creyghton, R. N. P.; De Franceschi, N.; Dekker, C.; Mulder, B. M.; Claassens, N. J.; ten Wolde, P. R.; van der Oost, J. Towards a Synthetic Cell Cycle. *Nat. Commun.* **2021**, *12*, Article number 4531.

(22) Schwille, P. Division in Synthetic Cells. *Emerg. Top. Life Sci.* **2019**, 3, 551-558.

(23) Deshpande, S.; Spoelstra, W. K.; Van Doorn, M.; Kerssemakers, J.; Dekker, C. Mechanical Division of Cell-Sized Liposomes. *ACS Nano* **2018**, *12,* 2560–2568.

(24) Litschel, T.; Ramm, B.; Maas, R.; Heymann, M.; Schwille, P. Beating Vesicles: Encapsulated Protein Oscillations Cause Dynamic Membrane Deformations. *Angew. Chemie - Int. Ed.* **2018**, *57*, 16286-16290.

(25) Oglęcka, K.; Rangamani, P.; Liedberg, B.; Kraut, R. S.; Parikh, A. N. Oscillatory Phase Separation in Giant Lipid Vesicles Induced by Transmembrane Osmotic Differentials. *Elife* **2014**, *3*, e03695.

(26) Karimi, M.; Steinkühler, J.; Roy, D.; Dasgupta, R.; Lipowsky, R.; Dimova, R. Asymmetric Ionic Conditions Generate Large Membrane Curvatures. *Nano Lett.* **2018**, 18, 7816-7821.

(27) Zwicker, D.; Seyboldt, R.; Weber, C. A.; Hyman, A. A.; Jülicher, F. Growth and Division of Active Droplets Provides a Model for Protocells. *Nat. Phys.* **2017**, *13*, 408-413.

(28) Levy, S.; Chevion, M. Synergistic Cytotoxic Effect of Tetrachlorocatechol and Sodium Azide in Escherichia Coli: Toxicity, Metabolism, and Mechanistic Aspects. *Environ. Toxicol. Chem.* **2009**, *28*, 1380-1389.

(29) Spahn, C.; Grimm, J. B.; Lavis, L. D.; Lampe, M.; Heilemann, M. Whole-Cell, 3D, and Multicolor STED Imaging with Exchangeable Fluorophores. *Nano Lett.* **2019**, *19*, 500-505.

(30) Zhao, H.; Shaqfeh, E. S. G. The Shape Stability of a Lipid Vesicle in a Uniaxial Extensional Flow. *J. Fluid Mech.* **2013**. https://doi.org/10.1017/jfm.2013.10.

(31) Narsimhan, V.; Spann, A. P.; Shaqfeh, E. S. G. The Mechanism of Shape Instability for a Vesicle in Extensional Flow. *J. Fluid Mech.* **2014**. *750*, 144-190.

(32) Tsai, H. H. G.; Lai, W. X.; Lin, H. Da; Lee, J. Bin; Juang, W. F.; Tseng, W. H. Molecular Dynamics Simulation of Cation-Phospholipid Clustering in Phospholipid Bilayers: Possible Role in Stalk Formation during Membrane Fusion. *Biochim. Biophys. Acta - Biomembr.* **2012**, *1818*, 2742-2755.

(33) Zhu, T. F.; Szostak, J. W. Exploding Vesicles. *J. Syst. Chem.* **2011**, *2*, Article number 4.

(34) Angelova, M. I.; Hristova, N.; Tsoneva, I. DNA-Induced Endocytosis upon Local Microinjection to Giant Unilamellar Cationic Vesicles. *Eur. Biophys. J.* **1999**, *28*, 142–150.

(35) Kawai, Y.; Mercier, R.; Wu, L. J.; Domínguez-Cuevas, P.; Oshima, T.; Errington, J. Cell Growth of Wall-Free L-Form Bacteria Is Limited by Oxidative Damage. *Curr. Biol.* **2015**, *25*, 1613–1618.

(36) Oehler, D. Z.; Walsh, M. M.; Sugitani, K.; Liu, M.-C.; House, C. H. Large and Robust Lenticular Microorganisms on the Young Earth. *Precambrian Res.* **2017**, *296*, 112–119.

(37) Dodd, M. S.; Papineau, D.; Grenne, T.; Slack, J. F.; Rittner, M.; Pirajno, F.; O'Neil, J.; Little, C. T. S. Evidence for Early Life in Earth's Oldest Hydrothermal Vent Precipitates. *Nature* **2017**, *543*, 60–64.

(38) Hutchison, C. A.; Chuang, R. Y.; Noskov, V. N.; Assad-Garcia, N.; Deerinck, T. J.; Ellisman, M. H.; Gill, J.; Kannan, K.; Karas, B. J.; Ma, L.; Pelletier, J. F.; Qi, Z. Q.; Richter, R. A.; Strychalski, E. A.; Sun, L.; Suzuki, Y.; Tsvetanova, B.; Wise, K. S.; Smith, H. O.; Glass, J. I.; Merryman, C.; Gibson, D. G.; Venter, J. C. Design and Synthesis of a Minimal Bacterial Genome. *Science.* **2016**, 351, 6280.

(39) Ruiz-Herrero, T.; Fai, T. G.; Mahadevan, L. Dynamics of Growth and Form in Prebiotic Vesicles. *arXiv Prepr. arXiv1901.04406* **2019**.

(40) Miller, S. L. A Production of Amino Acids under Possible Primitive Earth Conditions. *Science.* **1953**, *117*, 528–529.

(41) Szostak, J. W. The Narrow Road to the Deep Past: In Search of the Chemistry of the Origin of Life. *Angew. Chemie Int. Ed.* **2017**, *56*, 11037–11043.

(42) Budin, I.; Szostak, J. W. Physical Effects Underlying the Transition from Primitive to Modern Cell Membranes. *Proc. Natl. Acad. Sci.* **2011**, *108*, 5249–5254.

(43) Jordan, S. F.; Nee, E.; Lane, N. Isoprenoids Enhance the Stability of Fatty Acid Membranes at the Emergence of Life Potentially Leading to an Early Lipid Divide. *Interface Focus* **2019**, *9*, 20190067.

(44) Jordan, S. F.; Rammu, H.; Zheludev, I. N.; Hartley, A. M.; Maréchal, A.; Lane, N. Promotion of Protocell Self-Assembly from Mixed Amphiphiles at the Origin of Life. *Nat. Ecol. Evol.* **2019**, *3*, 1705-1714.

(45) Spitzer, J.; Poolman, B. The Role of Biomacromolecular Crowding, Ionic Strength, and Physicochemical Gradients in the Complexities of Life's Emergence. *Microbiol. Mol. Biol. Rev.* **2009**, *73*, 371–388.

(46) Hargreaves, W. R.; Mulvihill, S. J.; Deamer, D. W. Synthesis of Phospholipids and Membranes in Prebiotic Conditions. *Nature*. **1977,** 266, 78-80.

(47) Walsh, M. M.; Lowe, D. R. Filamentous Microfossils from the 3,500-Myr-Old Onverwacht Group, Barberton Mountain Land, South Africa. *Nature* **1985**, *314*, 530.

(48) Wacey, D.; Kilburn, M. R.; Saunders, M.; Cliff, J.; Brasier, M. D. Microfossils of Sulphur-Metabolizing Cells in 3.4-Billion-Year-Old Rocks of Western Australia. *Nat. Geosci.* **2011**, *4*, 698–702.

(49) Wacey, D.; Saunders, M.; Brasier, M. D.; Kilburn, M. R. Earliest Microbially Mediated Pyrite Oxidation In~ 3.4 Billion-Year-Old Sediments. *Earth Planet. Sci. Lett.* **2011**, *301*, 393–402.

(50) Lepot, K.; Williford, K. H.; Ushikubo, T.; Sugitani, K.; Mimura, K.; Spicuzza, M. J.; Valley, J. W. Texture-Specific Isotopic Compositions in 3.4 Gyr Old Organic Matter Support Selective Preservation in Cell-like Structures. *Geochim. Cosmochim. Acta* **2013**, *112*, 66–86.

(51) Kanaparthi, D.; Lampe, M.; Zhu, B.; Boesen, T.; Klingl, A.; Schwille, P.; Lueders, T. On the Nature of the Earliest Known Lifeforms. *bioRxiv* **2021**, 2021.08.16.456462.